Energy Conversion and Management 50 (2009) 885–892

Contents lists available at ScienceDirect

Energy Conversion and Management

journal homepage: www.elsevier.com/locate/enconman

Nonlinear control with wind estimation of a DFIG variable speed wind turbine for power capture optimization

B. Boukhezzar [a,*], H. Siguerdidjane [b,*]

[a] GREYC Control Team, 6 bd du Maréchal Juin, 14050 Caen, Cedex, France
[b] Automatic Control Department, Supélec, Plateau du Moulon, 3, Rue Joliot-Curie, 91192 Gif-sur-Yvette, Cedex, France

ARTICLE INFO

Article history:
Received 27 May 2008
Accepted 2 January 2009
Available online 8 February 2009

Keywords:
DFIG
Nonlinear control
Variable speed wind turbines
Wind speed estimation

ABSTRACT

A cascaded nonlinear controller is designed for a variable speed wind turbine equipped with a Doubly Fed Induction Generator (DFIG). The main objective of the controller is wind energy capture optimization while avoiding strong transients in the turbine components and specially in the drive train. The inner loop controller ensures an efficient tracking of both generator torque and stator flux, while the outer loop controller achieves a close tracking of the optimal blade rotor speed to optimize wind energy capture. It is combined to a wind speed estimator that provides an estimation of the wind speed and the aerodynamic torque involved in the controller. The global controller is firstly tested with a simplified mathematical model of the aeroturbine and DFIG for a high-turbulence wind speed profile. Secondly, the aeroturbine controller is validated upon a flexible wind turbine simulator. These new control strategies are compared to other existing controllers based on tests upon an aeroelastic wind turbine simulator. The obtained results show better performance in comparison with the existing controllers.

1. Introduction

Wind energy conversion systems have quickly evolved over the last decades, therefore, an efficient and reliable exploitation tools are necessary to make these installations more profitable [1]. It was shown that the control strategies have a major effect on the wind turbine and the electric grid loads [2], and whatever the kind of the wind turbine, the control strategy remains a key factor [3]. Modern high-power wind turbines (WT) are equipped with adjustable speed generators [4]. The doubly fed induction generator (DFIG) with a power converter is a common and efficient configuration to transfer the mechanical energy from the variable speed rotor to a constant frequency electrical grid [5]. Many contributions have been devoted to the control of the aeroturbine mechanical as well as the electrical components. The global control objective mainly consists in optimizing the extracted aerodynamic power in partial load area.

The contribution of this paper consists on proposing a new control structures even for the DFIG and the mechanical part (aeroturbine) that overcomes some of the drawbacks of existing control methods. The global controller is organized in two cascaded controllers. The first one concerns the aeroturbine, while the second one is devoted to the DFIG. These controllers are designed using the dynamical features of the wind speed, the aeroturbine and the DFIG together with their nonlinear characteristics.

Many approaches have been proposed for DFIG torque and flux control [6,7]. They are generally based on simplifying assumptions that allow the use of a vector control techniques similar to those employed with an induction machine control [8]. In order to achieve high-performance control during the transient period, a new DFIG controller is proposed. It consists on using a field oriented technic without any simplifications in the DFIG model.

For the aeroturbine mechanical part control, the control design is generally based on a local linearized model of the WT around its operating points [9]. Some nonlinear controllers were proposed assuming that the wind turbine operates in steady state conditions [10,11]. The dynamical aspect of the wind and the turbine is then not taken into consideration. The second contribution of this work then consists then on proposing an aeroturbine controller that is based directly on the nonlinearity and dynamics of the mathematical model without any need of wind speed measurement. The controller is also able to reject the effect of an additive disturbance on the control input.

The linearization by feedback is well known in the theory of nonlinear control systems, but in renewable energy domain, the classical controllers are mainly implemented only. In our previous works, we have proposed the use of the linearization by feedback based approach and also the use of LQG controller described in [12], with no consideration of DFIG.

* Corresponding authors. Tel.: +33 1 69 85 19 70; fax: +33 1 69 85 13 89 (B. Boukhezzar), tel.: +33 1 69 85 13 77; fax: +33 1 69 85 13 89 (H. Siguerdidjane).
E-mail addresses: boubekeur.boukhezzar@greyc.ensicaen.fr, b_boukhezzar@hotmail.com (B. Boukhezzar), houria.siguerdidjane@supelec.fr (H. Siguerdidjane).

0196-8904/$ - see front matter © 2009 Elsevier Ltd. All rights reserved.
doi:10.1016/j.enconman.2009.01.011

This paper is organized as follows: the aeroturbine and DFIG mathematical models are presented in Section 2. Section 3 starts with a description of the global control structure including the aeroturbine control and the DFIG control loops. The control objectives are then detailed. After a short review of some existing controllers, the proposed DFIG controlled is exposed in Section 4. The designed nonlinear static state feedback linearization with asymptotic rotor speed reference tracking and PI action are described in Section 5 in order to reach the required specifications for aeroturbine control. In Section 6, a brief description of the used aeroturbine simulator and the experimental wind turbine characteristics are given. After what, the validation results show quite good performance of the proposed approach upon the whole wind energy system.

2. Wind turbine modelling

2.1. Aeroturbine modelling

The aerodynamic torque expression is given by

$$T_a = \frac{1}{2}\rho\pi R^3 C_q(\lambda,\beta)v^2 \tag{1}$$

The torque coefficient C_q depends on the blade pitch angle β and the tip-speed ratio λ which is defined as follows:

$$\lambda = \frac{\omega_t R}{v} \tag{2}$$

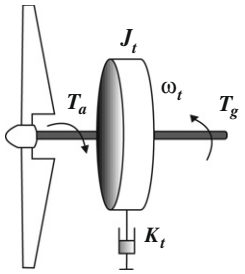

Fig. 1. One mass wind turbine model dynamics.

where ω_t is the rotor speed, R is the rotor radius and ρ is the air density.

If a perfectly rigid low-speed shaft is assumed, a single mass model of the turbine may then be considered [13]

$$J_t\dot{\omega}_t = T_a - K_t\omega_t - T_g \tag{3}$$

where

$$J_t = J_r + n_g^2 J_g$$
$$K_t = K_r + n_g^2 K_g$$
$$T_g = n_g T_{em}$$

The one mass wind turbine model is shown in Fig. 1.

2.2. DFIG modelling

A scheme of a DFIG-based wind turbine is shown in Fig. 2. This kind of wound-rotor machine can be fed from both stator and rotor side [14]. The most significant feature of the DFIG is that the stator is directly connected to the grid while the rotor winding is interfaced through a back-to-back variable frequency, voltage source converters [4]. By decoupling the power system electrical frequency and the rotor mechanical frequency, the converter system allows a variable speed operation of the wind turbine. As commonly done in the literature [15], the DFIG is described in the *Park d–q* frame by the well known following set of equations:

$$v_{sd} = R_s\cdot i_{sd} + \frac{d\Phi_{sd}}{dt} - \omega_s\cdot\Phi_{sq} \tag{4}$$
$$v_{sq} = R_s\cdot i_{sq} + \frac{d\Phi_{sq}}{dt} + \omega_s\cdot\Phi_{sd} \tag{5}$$
$$v_{rd} = R_r\cdot i_{rd} + \frac{d\Phi_{rd}}{dt} - \omega_r\cdot\Phi_{rq} \tag{6}$$
$$v_{rq} = R_r\cdot i_{rq} + \frac{d\Phi_{rq}}{dt} + \omega_r\cdot\Phi_{rd} \tag{7}$$

As the d and q axis are magnetically decoupled, the flux are given by

$$\Phi_{sd} = L_s\cdot i_{sd} + M\cdot i_{rd} \tag{8}$$
$$\Phi_{sq} = L_s\cdot i_{sq} + M\cdot i_{rq} \tag{9}$$
$$\Phi_{rd} = L_r\cdot i_{rd} + M\cdot i_{sd} \tag{10}$$
$$\Phi_{rq} = L_r\cdot i_{rq} + M\cdot i_{sq} \tag{11}$$

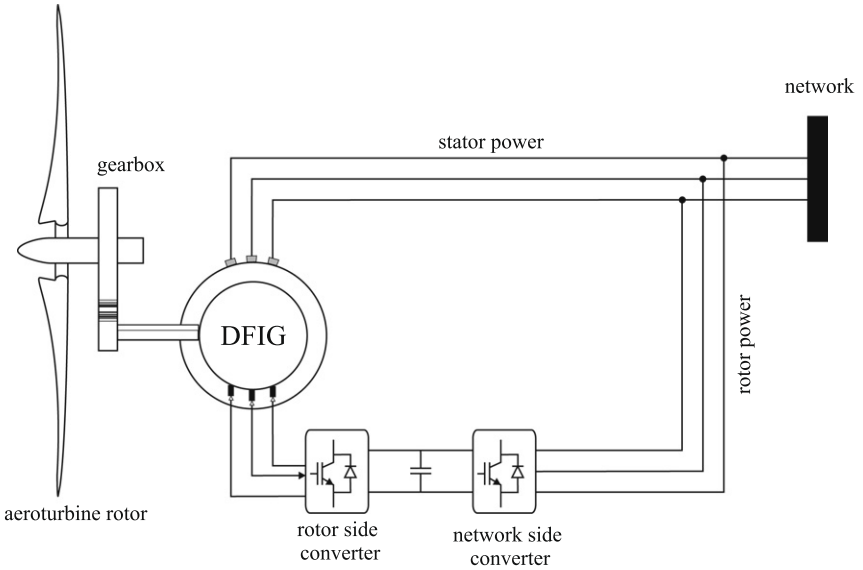

Fig. 2. Configuration scheme of a DFIG-based wind turbine.

for the reader convenience, the list of symbols is given in Appendix A.

3. Control problem formulation

3.1. Control structure

The WT electric system time responses are much faster than those of the other parts of the WT. This makes it possible to dissociate the generator and the aeroturbine control designs and thus define a cascaded control structure around two control loops:

(1) The inner control loop concerns the electric generator via the power converters.
(2) The outer control loop concerns the aeroturbine that provides the reference inputs of the inner loop.

Thereafter, these two control levels will be considered separately. As seen in Fig. 3, the DFIG controller is considered as a low level one.

We will describe the two level controllers in the following sections.

3.2. Control objectives

The objective of this work is first to design a vector controller of the DFIG without any reducing assumptions in its mathematical model and second to design a nonlinear controller of the aeroturbine that takes into consideration the dynamical aspect of the wind speed and the mechanical part, its nonlinear characteristic, without a need of wind speed measurement.

The objective of the aeroturbine controller is to optimize wind power capture. The aerodynamic power captured by the aeroturbine rotor is given by

$$P_a = \frac{1}{2}\rho\pi R^2 C_p(\lambda,\beta)v^3 \tag{12}$$

The $C_p(\lambda,\beta)$ curve is specific for each wind turbine. It has a unique maximum $C_{p_{opt}}$ at a single point

$$C_p(\lambda_{opt},\beta_{opt}) = C_{p_{opt}} \tag{13}$$

In order to maintain λ at its optimal value for a given wind speed v, the rotor speed must be adjusted using the generator torque to track the reference $\omega_{t_{opt}} = \frac{\lambda_{opt}}{R}v$.

The system output to be controlled is the rotor speed ω_t and the control problem is the tracking of an optimal rotor speed reference $\omega_{t_{opt}}$ that ensures maximum wind power capture. Notice that the blade pitch angle could be used as an additional control input to achieve electrical power regulation, for high-wind speeds.

The main objectives of the DFIG controller are:

- Regulate the stator flux to its nominal value Φ_{ref}.
- Track the generator reference torque $T_{g_{ref}}$ that is the aeroturbine control input.

4. DFIG control design

For the DFIG control, classical techniques as vector control were extensively used [6,16]. In most cases, the proposed control strategies are derived from those used with an induction machine using simplifying assumptions on the DFIG model. For this purpose, many kinds of assumptions can be found in the literature: either the rotor and stator transients are neglected [17], either the rotor currents are assumed to be previously controlled [18], or the stator resistance voltage loss [19,20] neglected. A reduced order dynamic DFIG model is then used for controller design.

In order to improve the transient behavior of the controllers, it is more convenient to use a complete model of the DFIG. To achieve this objective, a new vector control technic based on the DFIG model, without any reduction, is presented as a first contribution in this paper.

To make the stator flux in quadrature with the q axis, the Park frame is oriented such that

$$\Phi_{sd} = \Phi_{ref} \tag{14}$$
$$\Phi_{sq} = 0 \tag{15}$$

The stator and rotor voltages (4)–(7) are then simplified to [15]

$$v_{sd} = -\frac{M}{T_s}\cdot i_{rd} + \left(\frac{1}{T_s}+s\right)\cdot\Phi_{sd} \tag{16}$$
$$v_{sq} = -\frac{M}{T_s}\cdot i_{rq} + \omega_s\cdot\Phi_{sd} \tag{17}$$
$$v_{rd} = v'_{rd} + e_d \tag{18}$$
$$v_{rq} = v'_{rq} + e_q \tag{19}$$

with

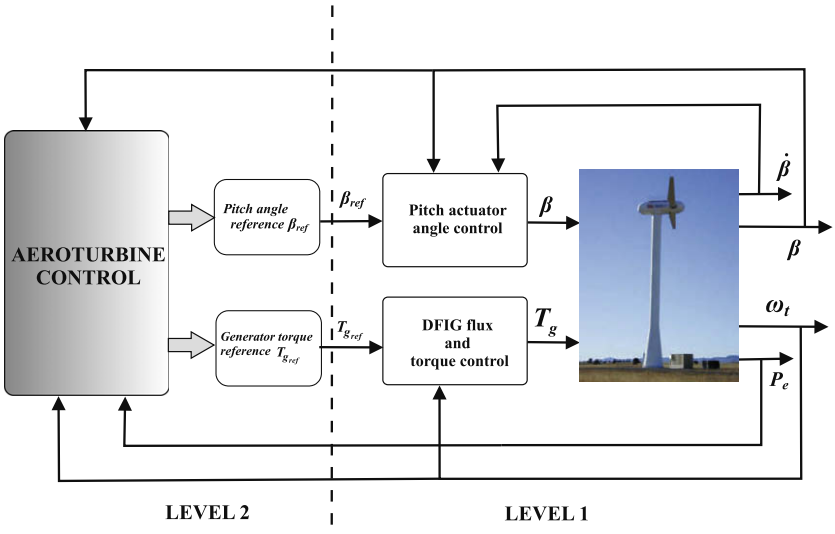

Fig. 3. Wind turbine control levels.

$$v'_{rd} = (R_r + L_r\sigma s)\cdot i_{rd} \quad (20)$$

$$v'_{rq} = (R_r + L_r\sigma s)\cdot i_{rq} \quad (21)$$

and

$$e_d = -L_r\omega_r\sigma\cdot i_{rq} \quad (22)$$

$$e_q = L_r\omega_r\sigma\cdot i_{rd} + \frac{M}{L_s}\omega_r\cdot\Phi_{sd} \quad (23)$$

$\sigma = 1 - \frac{M^2}{L_r L_s}$ is the scattering coefficient, T_s the rotor time constant and s the Laplace variable.

Using (16) and (5), we deduce an estimate of the stator flux and ω_s frequency

$$\hat{\Phi}_{sd} = \frac{T_s}{1+T_s s}\cdot v_{sd} + \frac{M}{1+T_s s}\cdot i_{rd} \quad (24)$$

$$\hat{\omega}_s = \frac{v_{sq} - R_s\cdot i_{sq}}{\hat{\Phi}_{sd}} \quad (25)$$

$$\hat{\omega}_r = \hat{\omega}_s - p\cdot\omega_t \quad (26)$$

From (20), it may be seen that the d component of the rotor current i_{rd} can be set to $i_{rd_{ref}}$ via v'_{rd} using a PI regulator and the decoupling term e_d.

The $i_{rd_{ref}}$ is the input of the flux subsystem

$$\hat{\Phi}_{sd} = \frac{M}{1+T_s s}\cdot i_{rd_{ref}} + \frac{T_s}{1+T_s s}\cdot v_{sd} \quad (27)$$

The second term $\frac{T_s}{1+T_s s}\cdot v_{sd}$ can be seen as an output disturbance and compensated using an appropriate regulator that generates $i_{rd_{ref}}$ [21].

Once Φ_{sd} assigned to Φ_{ref}, the generator torque will only depend on i_{rq} via v'_{rq}

$$T_g = -\frac{pM\Phi_{ref}}{L_s}\cdot\frac{1}{R_r + L_r\sigma s}\cdot v'_{rq} \quad (28)$$

a PI regulator is also sufficient to regulate T_g via v'_{rq} and the decoupling term e_q. The global DFIG control scheme is shown in Fig. 4.

5. Nonlinear static state feedback linearization with PI action and estimator

A nonlinear static state feedback linearization with asymptotic rotor speed reference tracking and estimator was proposed in [22] for wind turbine power capture optimization. In addition to the aerodynamic torque estimate, the estimator gives also an estimate of the rotor speed $\hat{\omega}_t$ and the effective wind speed $\hat{v}$ (Fig. 5).

As mentioned in [23], using the following control torque

$$T_g = T_a - K_t\omega_t - J_t a_0\varepsilon - J_t\dot{\omega}_{t_{opt}} \quad (29)$$

A first order dynamic response is imposed for the rotor speed tracking error

$$\dot{\varepsilon} + a_0\varepsilon = 0, \quad a_0 > 0 \quad (30)$$

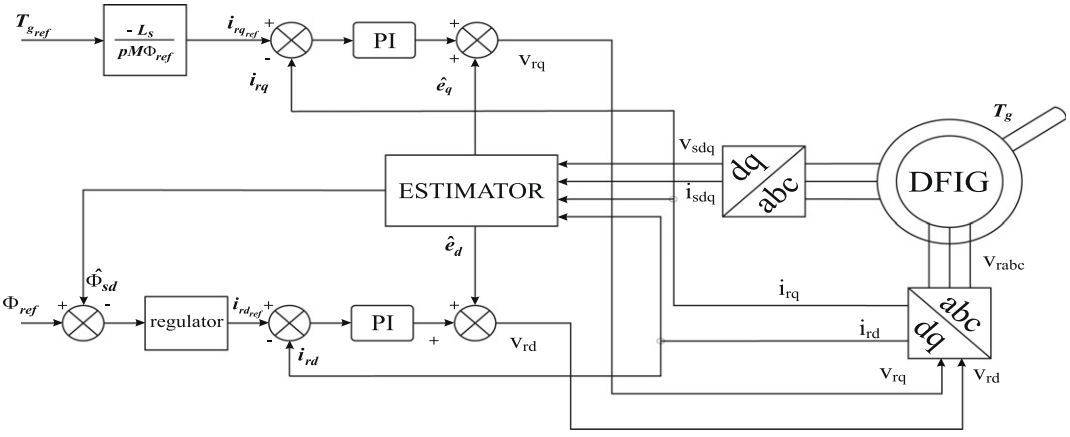

Fig. 4. DFIG control scheme.

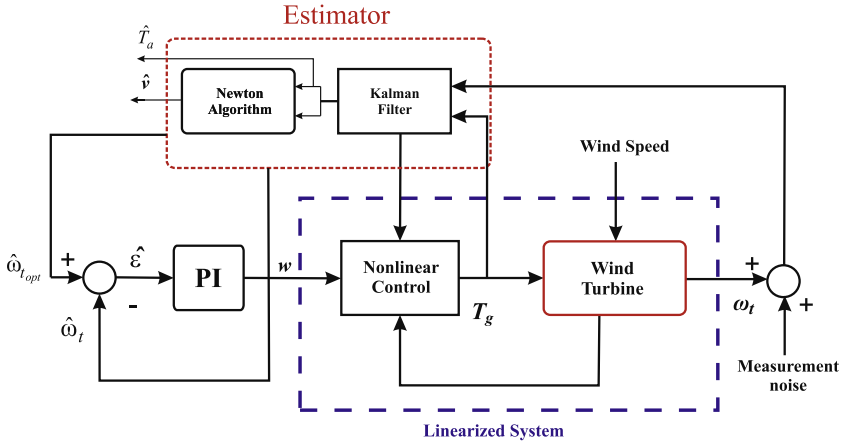

Fig. 5. Nonlinear state space feedback linearization with PI controller and wind speed estimator.

where

$$\hat{\varepsilon} = \hat{\omega}_{t_{opt}} - \hat{\omega}_t \tag{31}$$

This technique is known to lack robustness with respect to perturbations [24].

In order to improve controller performance in presence of additive disturbance, a nonlinear state feedback with PI controller is developed next. Even if a nonlinear state feedback with a higher order asymptotic tracking dynamic can reject the effect of input disturbance, it will introduce a more complex control law that will contain also higher order derivatives [22,23]. The implementation of the control algorithm can then be difficult due to numerical derivation sensitivity to noise in the measured signal. Another approach is proposed herein based on the use of classical linear controllers upon the linearized system using the nonlinear state feedback.

If we consider the behavior Eq. (3) with the control torque

$$T_g = J_t\left[\frac{\hat{T}_a}{J_t} - \frac{K_t}{J_t}\omega_t - w\right] \tag{32}$$

this system can be seen as a simple integrator with input w

$$\dot{\omega}_t = w$$

linear control technique can then be used for optimal rotor speed tracking.

A PI controller is then used to track the optimal speed $\hat{\omega}_{t_{opt}}$ deduced from estimated wind speed $\hat{v}$.

$$w(t) = K\left[\hat{\varepsilon}(t) + \frac{1}{T_i}\int_0^t \hat{\varepsilon}(\tau)d\tau\right] \tag{33}$$

where $\hat{\varepsilon}$ is the estimated tracking error given in (31).

The global controller scheme using the estimator and the PI controller upon the nonlinear feedback linearization wind turbine is shown in Fig. 5. Finally, the control torque T_g is given by

$$T_g = J_t\left[\frac{\hat{T}_a}{J_t} - \frac{K_t}{J_t}\omega_t - K\left(\hat{\varepsilon}(t) + \frac{1}{T_i}\int_0^t \hat{\varepsilon}(\tau)d\tau\right)\right] \tag{34}$$

Since the integral action is used to cancel the steady state error only, so the integration constant is chosen in such a way that $\frac{1}{T_i}$ is far away from the system bandwidth. The adequate value of K is 49×10^3.

6. Validation results

The proposed aeroturbine controller was validated using the FAST (Fatigue, Aerodynamics, Structures and Turbulence) aeroelastic simulator (see next section) with the parameters of the Controls Advanced Research Turbine (CART) which is located at NREL.[1] Its detailed characteristics can be found in [25]. The CART is a variable speed, variable pitch WT with a nominal power rating of 600 kW and a hub height of 36 m. It is a 43-m diameter, two-bladed, teetered hub machine. It is assumed to be coupled to a three-phase DFIG. The characteristics are given in [26]. The main parameters of CART are summarized in Table 1.

6.1. FAST aeroelastic simulator description

FAST code is developed by NREL [27]. It is an aeroelastic WT simulator capable of modelling two and three bladed propeller-type machines. This code is used by WT designers to predict both extreme and fatigue loads. FAST was evaluated and recommended by Germanischer Lloyd WindEnergie to calculate onshore wind turbine loads for design and certification [28].

Table 1
Wind turbine characteristics.

Rotor diameter	43.3 m
Gearbox ratio	43.165
Hub-height	36.6 m
Generator system electrical power	600 kW
Maximum rotor torque	162 kN m

It uses an assumed mode method to model flexible blades and tower components. Other components are modelled as rigid bodies. In this study, three degrees-of-freedom (DOFs) are simulated: the variable generator and rotor speed (two DOFs) and the blade teeter DOF. The variable generator and rotor speed DOFs account for the variations in generator speed and the drive train flexibility associated with torsional motion between the generator and hub/rotor. The blade teetering DOF accounts for the teeter motion induced by asymmetric wind loads across the rotor plane. FAST subroutines are coupled in an S-Function to be incorporated in a Simulink model. Hence, FAST is interfaced with Matlab Simulink allowing users to develop and test high-performance controllers.

6.2. Simulating environment

The full-field turbulent wind set v used in this study is generated using SNwind [29] developed by NREL and coupled with FAST. The hub-height wind speed profile is illustrated in Fig. 6. It has a mean value of 7 m s^{-1} at the hub-height and a turbulence intensity of 25%.

The main control objective is to maximize the captured energy from the wind while limiting the transient loads experienced by the turbine (see Section 3). Transient loads reduction amounts mainly to low-speed shaft torsion minimizing, which is equivalent to reducing the variance of the high-speed shaft torsional moment. The generator torque and the rotor speed must also be both within the required constraints of 162 kN m and 58 rpm [30], respectively.

To get more realist operating conditions, an additive measurement noise on ω_t has been introduced. The Signal to Noise Ratio (SNR) is approximately 7 dB. This is a band-limited, white noise. A constant additive disturbance d of 10 kN m is also introduced on the control torque T_g. A common phenomenon that can correspond to a constant additive disturbance on the generator torque is the static friction that can be considered as unknown and constant additive torque or a bias on the generator torque controller. Therefore, such kind of disturbance is chosen.

6.3. DFIG controller validation

The low level DFIG controller performance are first investigated. As seen in Fig. 7a, the stator flux Φ_{sd} reachs the constant desired reference Φ_{ref} in less than 10 ms. The DFIG torque T_g is then independently controlled to track the reference torque $T_{g_{ref}}$. The torque controller achieves good performance while T_g and $T_{g_{ref}}$ exhibit almost the same behavior (Fig. 7b).

These results proof the ability of the proposed DFIG controller to achieve high-level performance during the transient period. This is due to the fact that no assumption is made on the DFIG model during the controller synthesis as the neglected terms can have a significant influence during this phase.

6.4. Validation using FAST

The proposed nonlinear state feedback-PI with estimator (NSFE-PI) controller is implemented as well as existing controllers for comparison using the FAST wind turbine dynamic simulation.

[1] NREL (National Renewable Energy Laboratory), Golden, CO.

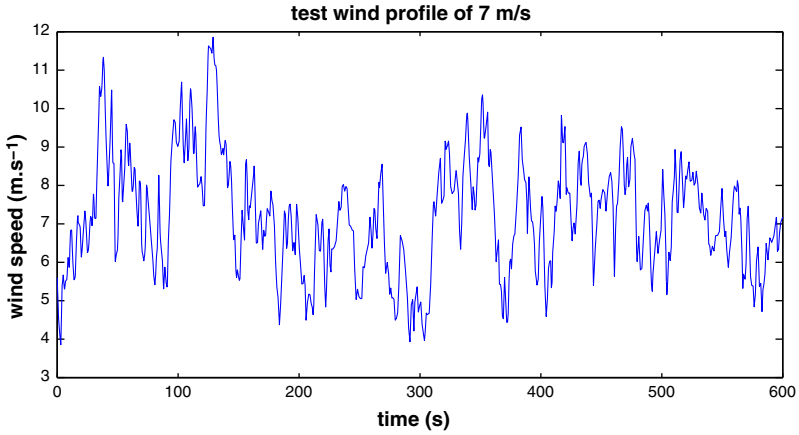

Fig. 6. Wind speed profile of 7 m s^{-1} mean value.

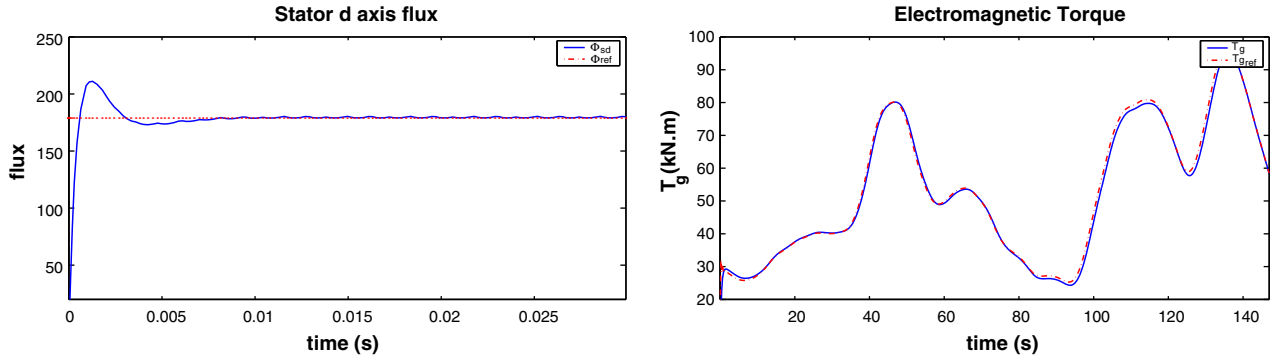

(a) Stator flux (b) Generator torque

Fig. 7. DFIG controller performance.

Fig. 8a–d compares the performance obtained using the nonlinear static state feedback with asymptotic error tracking (NSSFET) and the proposed controller. The NSSFET controller is obviously unable to reject the unknown disturbance applied to the control input (Fig. 8a). This causes the deviation of the rotor speed from its optimal reference. The deviation is more visible in between 250 and 400 s. In spite of the presence of the disturbance, the nonlinear state feedback-PI controller with estimator succeeded in keeping the rotor speed around of the optimal reference speed (Fig. 8a). One may observe in Fig. 8b that the control torque used in the NSFE-PI controller to reject the additive disturbance is more important than that developed in the NSSFET. However, it still remains below the upper bound, though. The disturbance rejection results in an increase of the captured energy for the NSFE-PI controller compared to the nonlinear static state feedback one (Fig. 8c). As seen in Fig. 8a, the rotor speed tracks mean tendency of the optimal rotational speed. That causes its variations to remain smooth. The differences between the optimal rotor speed reference and rotor speed occur during the start-up transient. The generator torque from the FAST model (Fig. 8b) is greater than that obtained with the mathematical model while remaining below the maximum acceptable value. Inversely, the electrical power produced is less than the one given by the simplified mathematical model (Fig. 8c). This decrease can be interpreted by the highest complexity of the wind turbine simulator that includes more flexible elements and consequently induces more power losses than the simplified mathematical model.

The efficiency of the Kalman filter used with the Newton algorithm estimator can be seen in Fig. 8d. It provides a good estimate of the wind speed through the aerodynamic torque and rotor speed estimates even with the noisy measurements of ω_t and T_g. Concerning the control torque disturbance, it is only rejected with the nonlinear state feedback-PI controller with estimator. The NSSFET and NSFE-PI performance are compared with the two baseline controllers: the Indirect Speed Controller (ISC) [13] and the Aerodynamic Torque Feed Forward (ATF) control strategy [13].

The validation tests have been performed by using the wind turbine simulator FAST with the same wind speed profile under identical operating conditions concerning disturbance, and measurement noise.

The obtained performance with the different controllers are shown in Fig. 9 and summarized in Table 2. The selected comparison criteria are the power capture efficiency and the low-speed shaft torque torsional standard deviation. One can observe in Fig. 9a that the produced electric power using the NSFE-PI is a little bit more significant. The low-speed shaft torque oscillations are also shown to be reduced using this control strategy, as depicted in Fig. 9b. On the one hand, one may notice that the performance of the three first controllers remain close. On the other hand, one can note that the NSFE-PI controller with estimator allows an improvement of 18% of the efficiency compared to the indirect speed controller with a quietly similar standard deviation of the low-speed shaft torsional torque T_{ls}.

Both of the first three controllers are unable to reject the presence of the control input disturbance. As the ISC controller synthetized in steady state regime, it does not take into account the high-turbulence of the wind speed which leads to a decrease in power capture efficiency.

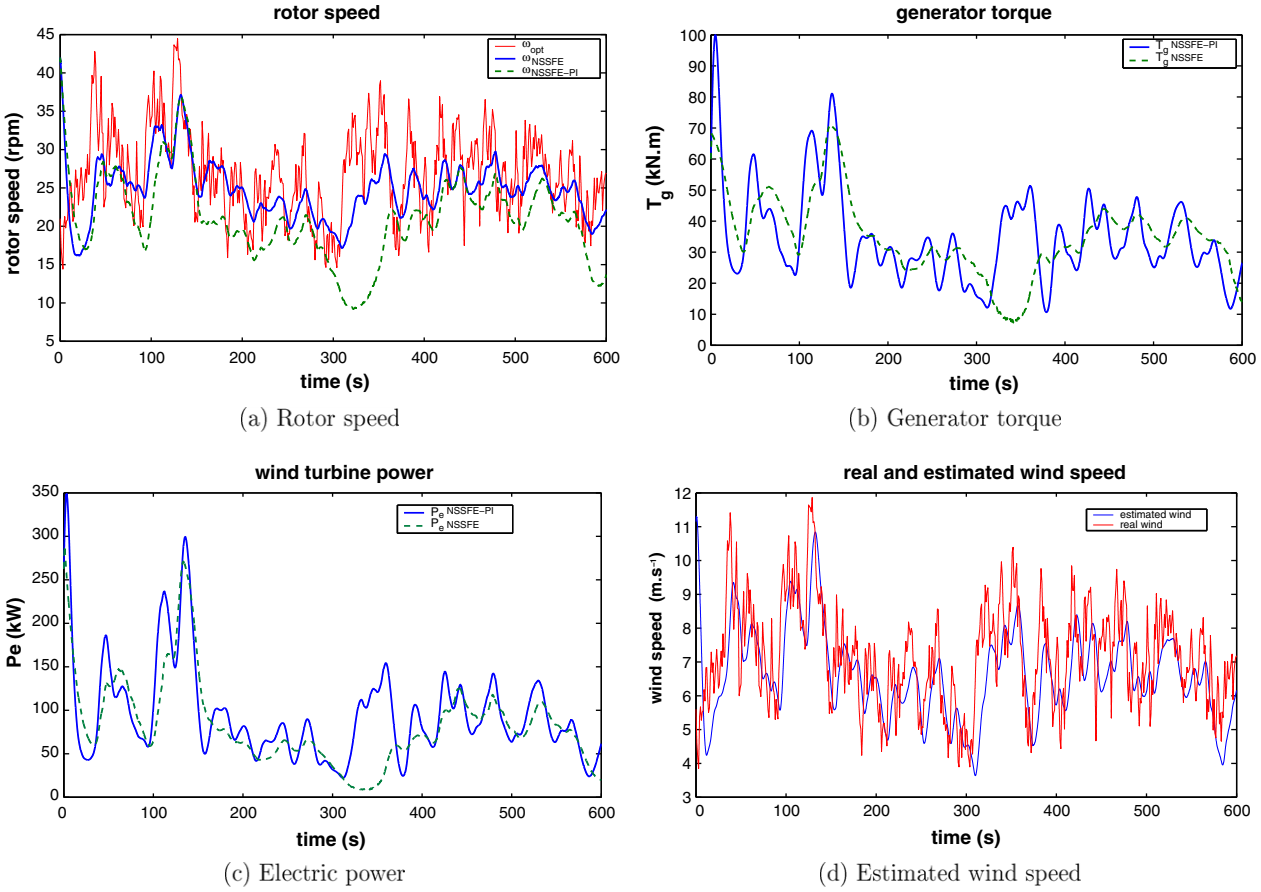

(a) Rotor speed (b) Generator torque

(c) Electric power (d) Estimated wind speed

Fig. 8. Nonlinear state feedback with asymptotic error tracking and PI action controllers, with estimator.

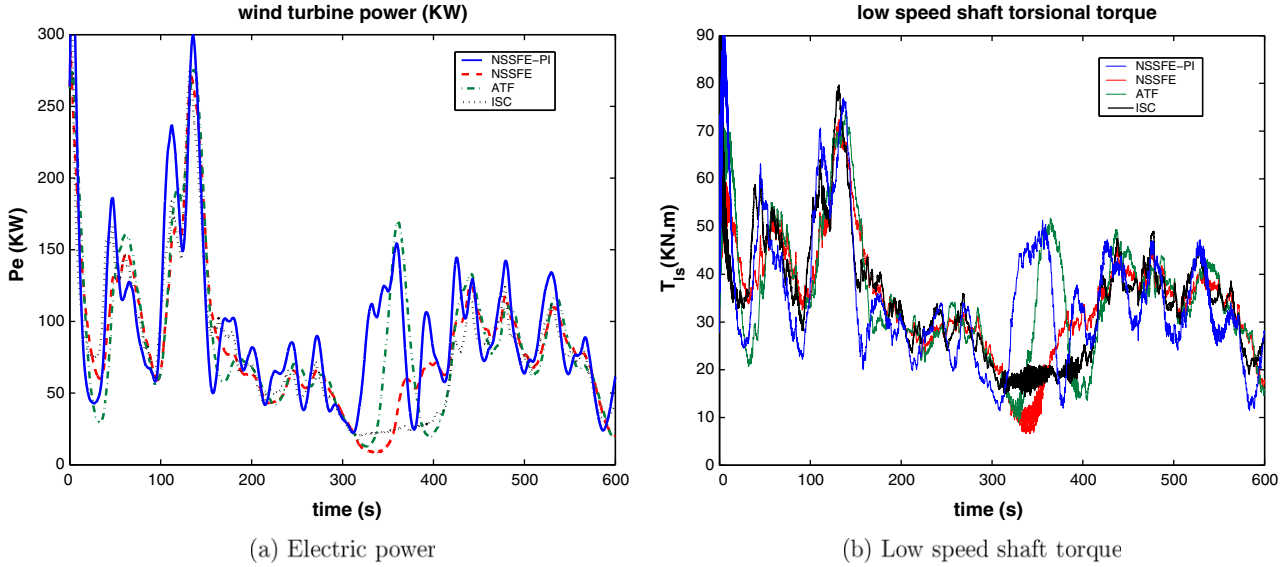

(a) Electric power (b) Low speed shaft torque

Fig. 9. Comparison of the different control strategies.

Table 2
Comparison of the different control strategies.

Controller	ISC	NSSFET	ATF	NSFE-PI
Efficiency (%)	51.79	61.23	63.43	70.00
$std(T_{hs})$ (kN m)	12.73	11.87	13.19	12.64
$\max(T_g)$ (kN m)	112.35	70.70	76.99	81.09

7. Conclusion

The presented research work deals with variable speed wind control design, in order to achieve the objectives of maximizing the extracted energy from the wind, below the rated power area. Cascaded two controllers have been suggested for both DFIG and aeroturbine control.

The proposed inner control loop concern the DFIG control. It achieves a good tracking of rotor reference flux and torque even during the transient phase. The uses of a nonlinear state feedback-PI controller jointly with an estimator for the aeroturbine outer control loop allow to take into consideration the dynamic aspect of the wind turbine, of its aerodynamic behavior nonlinearity and of the turbulent nature of the wind. This controller allows the rejection of the effect of the disturbance and achieved the goal.

The designed nonlinear state feedback-PI controller with estimator ensures the best performance in terms of efficiency with an acceptable drive train transient loads and better implementation simplicity compared to some existing controller strategies.

Appendix A. List of symbols

v	wind speed, m s^{-1}
ρ	air density, kg m^{-3}
R	rotor radius, m
P_a	aerodynamic power, W
T_a	aerodynamic torque, N m
λ	tip-speed ratio
β	pitch angle, deg
C_p	power coefficient
C_q	torque coefficient
ω_t	aeroturbine rotor speed, rad s^{-1}
T_{em}	DFIG torque, N m
T_g	DFIG torque in the rotor side, N m
T_{ls}	low-speed shaft torque, N m
T_{hs}	high-speed shaft torque, N m
J_r	rotor inertia, kg m^2
J_g	DFIG inertia, kg m^2
J_t	turbine total inertia, kg m^2
K_r	rotor external damping, N m rad^{-1} s
K_g	DFIG external damping, N m rad^{-1} s
K_t	total external damping, N m rad^{-1} s
K_{ls}	low-speed shaft damping, N m rad^{-1} s
n_g	gearbox ratio
P_e	electrical power, W
$v_{sd,q}$	stator d–q voltage, V
$v_{rd,q}$	rotor d–q frame voltage, V
$i_{sd,q}$	stator d–q frame current, A
$i_{rd,q}$	rotor d–q frame current, A
$\Phi_{rd,q}$	rotor d–q frame flux, Wb
$\Phi_{rd,q}$	rotor d–q frame flux, Wb
R_s	stator resistance, Ω
R_r	rotor resistance, Ω
L_s	stator inductance, H
L_r	rotor inductance, H
M	mutual inductance, H
σ	scattering coefficient
p	number of poles
ω_s	stator d–q reference axes speed, rad s^{-1}
ω_r	rotor d–q reference axes speed, rad s^{-1}

References

[1] Manwell JF, McGowan J, Rogers A. Wind energy explained: theory design and applications. John Wiley & Sons; 2002.

[2] Bianchi FD, Battista HD, Mantz RJ. Wind turbine control systems: principles modelling and gain scheduling design. 2nd ed. Springer; 2006.

[3] Burton T, Sharpe D, Jenkins N, Bossanyi E. Wind energy handbook. John Wiley & Sons; 2001.

[4] Muller S, Deicke M, De Doncker RW. Doubly fed induction generator systems for wind turbines. IEEE Ind Appl Mag 2002:26–33.

[5] Lindholm M. Doubly fed drives for variable speed wind turbines. Ph.D. thesis, Technical University of Denmark; 2004.

[6] Cardenas RJ, Pena RS, Asher J, Asher GM, Clare JC. Sensorless control of a doubly-fed induction generator for stand alone operation. In: IEEE 35th annual power electronics specialists conference, vol. 5; 2004. p. 3378–83.

[7] Pena RS, Cardenas RJ, Clare JC, Asher GM. Control strategy of doubly fed induction generators for a wind diesel energy system. In: IEEE 2002 28th annual conference of the industrial electronics society, vol. 4; 2002. p. 3297–302.

[8] Poitiers F, Machmoum M, Doeuff RL. Simulation of wind energy conversion system based on a doubly-fed induction generator. In: 10th European conference on power electronics and applications, CD-ROM proceedings, France, Toulouse; 2003.

[9] Ma X. Adaptive extremum control and wind turbine control. Ph.D. thesis, Denmark, May; 1997.

[10] Song YD, Dhinakaran B, Bao XY. Variable speed control of wind turbines using nonlinear and adaptive algorithms. J Wind Eng Ind Aerodynam 2000;85(3):293–308.

[11] Valenciaga F, Puleston PF. Variable structure control of a wind energy conversion system based on a brushless doubly fed reluctance generator. IEEE Trans Energy Convers 2007;22(2):499–506.

[12] Boukhezzar B, Lupu L, Siguerdidjane H, Hand M. Multivariable control strategy for variable speed variable pitch wind turbines. Renew Energy 2007;32(8):1273–87.

[13] Boukhezzar B. Sur les stratégies de commande pour l'optimisation et la régulation de puissance des eoliennes à vitesse variable, Ph.D. thesis, Université de Paris Sud-Supélec; February 2006.

[14] Tapia A, Tapia G, Ostolaza X, Sáenz JR. Modelling and control of a wind turbine driven doubly fed induction generator. IEEE Trans Energy Convers 2003;18(2):194–204.

[15] Aimani SE. Modélisation de différentes technologies d'éoliennes intégrées dans un réseau moyenne tension. Ph.D. thesis, Ecole Centrale de Lille-Université des Sciences et Technologies de Lille 1; December 2004.

[16] Hopfensberger B, Atkinson DJ, Lakin RA. Stator flux oriented control of a cascaded doubly-fed induction machine. IEE Proc – Electric Power Appl 1999:597–605.

[17] Slootweg JG, Polinder H, Kling WL. Dynamic modelling of a wind turbine with doubly fed induction generator. In: IEEE power engineering society summer meeting; 2001. p. 644–9.

[18] Forchetti D, Garcia G, Valla MI. Vector control strategy for a doubly-fed stand-alone induction generator. In: IEEE 2002 28th annual conference of the industrial electronics society; 2002. p. 991–5.

[19] Pena R, Clare JC, Asher GM. Doubly fed induction generator using back-to-back PWM converter and its application to variable-speed wind-energy generation. IEE Proc B 1996;143(3):231–41.

[20] Poitiers F, Machmoum M, Doeuff RL, Zaim M. Control of a doubly-fed induction generator for wind energy conversion systems. In: Proceedings of the Australasian Universities power engineering conference; 2001.

[21] Goodwin GC, Graebe SF, Salgado ME. Control system design. Prentice Hall; 2000.

[22] Boukhezzar B, Siguerdidjane H, Hand M. Nonlinear control of variable-speed wind turbines for generator torque limiting and power optimization. ASME J Solar Energy Eng 2006;128(4):516–30.

[23] Boukhezzar B, Siguerdidjane H. Nonlinear control of variable speed wind turbines without wind speed measurement. In: ECC-CDC 2005, Seville, Spain; 2005.

[24] Nijmeijer H, Schaft AVD. Nonlinear dynamical control systems. Springer-Verlag; 1996.

[25] Stol KA. Geometry and structural properties for the controls advanced researchturbine CART from model tuning. Subcontractor report SR-500-32087, National Renewable Energy Laboratory, Golden, Colorado; September 2004.

[26] Poitiers F, Machmoum M, Doeuff RL, Zaim M. Direct torque control of a doubly-fed induction generator for variable speed wind turbine power regulation. In: 2007 European wind energy conference proceedings, EWEA, Milan, Italy; 2007.

[27] Jonkman JM, Buhl ML. FAST user's guide. 6th ed. National Wind Technology Center, National Renewable Energy Laboratory, Golden, Colorado.

[28] Manjock A. Design codes fast and ADAMS® for load calculations of onshore wind turbines. NREL report 72042, Germanischer Lloyd WindEnergie GmbH, Hamburg, Germany.

[29] Buhl ML. SNwind user's guide. 1st ed. National Wind Technology Center, National Renewable Energy Laboratory, Golden, Colorado; June 2003.

[30] Fingersh LJ, Johnson K. Controls advanced research turbine (CART) commissioning and baseline data collection. NREL report TP-500-32879, National Renewable Energy Laboratory, Golden, Colorado; October 2002.